Eur. Phys. J. A (2023) 59:168
https://doi.org/10.1140/epja/s10050-023-01076-7

THE EUROPEAN PHYSICAL JOURNAL A

Regular Article - Experimental Physics

AGATA: Nuclear structure advancements with high-energy γ rays

F. Camera[1,2,a], **J. Isaak**[3,b], **A. Maj**[4,c], **S. Siem**[5,d]

[1] Dipartimento di Fisica, Università degli Studi di Milano, 20133 Milano, Italy
[2] INFN Sezione di Milano, 20133 Milano, Italy
[3] Institut für Kernphysik, Technische Universität Darmstadt, Schlossgartenstr. 9, 64289 Darmstadt, Germany
[4] Niewodniczanski Institute of Nuclear Physics PAN, Radzikowskiego 152, 31-342 Krakow, Poland
[5] Department of Physics, University of Oslo, Sem Sæland vei 22, 0316 Oslo, Norway

Received: 13 March 2023 / Accepted: 28 June 2023

Communicated by Nicolas Alamanos

Abstract High-energy γ rays are emitted either in the decay of nuclear discrete states (generally located in the proximity of the particle-emission threshold) or in the electromagnetic decay of collective states. The branching ratio is rather small, therefore in alternative/coincidence with high-energy γ rays one could have neutron or charged-particle emission. The precise measurement of these branching ratios allows a more comprehensive description of the nucleus and, in particular, the selection of the nuclear models which better describes the interplay between the different acting forces and couplings. In the case of the electromagnetic decay of collective states, the precise identification of the populated low-lying states allows the measurement of their wavefunction and/or of their 'bulk' properties. This information provides, also in this case, a stringent test for the nuclear models. In both cases, to compensate these small branching ratio, a large number of detectors and an accurate selection of a small region of the phase space are needed. AGATA is considered to constitute an optimal array for this kind of measurements. In fact, AGATA, because of its high granularity and its excellent energy resolution, can detect the high-energy γ rays emitted in a specific decay path or associated to specific reaction channels, shapes, deformations. In the introduction, some details on the measurement of high-energy γ rays using HPGe detector are discussed. The sections of this paper focus on the measurements of high-energy γ rays to obtain the photon strength function, the nuclear level density and to identify extreme shapes in highly excited nuclei.

1 Introduction: high-energy γ-ray detection

It is well known that the probability of interaction of γ radiation in matter mainly depends on both the atomic number and volume of the detector, its density and, obviously, on the energy of the γ radiation. Therefore, the measurement of high-energy γ rays is usually performed with inorganic, large volume fast scintillators because of their larger full-energy peak efficiency and excellent time resolution. However, in some cases, AGATA, with its segmented HPGe, can provide an equal, if not better, information. In other cases AGATA will offer a possibilities to set very clean conditions (gates) on discrete transitions, without which obtaining informations from the scintillator spectra will be not possible.

Each AGATA crystal has a dimension (it can be described approximately as a cylinder 9 cm long and 8 cm large with a central hole 1 cm large and 8 cm long) that can fully stop most of the low-energy γ rays and some of the medium energy ones (in general, those which mainly interact through Compton or photoelectric interaction). As the energy of the γ radiation (e.g. $E_\gamma > 6$ MeV) increases, the average depth of the first interaction increases and, for γ radiation of the order of 15 MeV, it reaches a depth of approximately 10 cm.

The efficiency of a large volume scintillator array is, therefore, expected to be higher than that of AGATA simply because the active volume of a scintillator can be much larger than that of HPGe crystal. An estimate of the efficiency of GRETA at 15 MeV was published in Ref. [4]. It was estimated to be of the order of 2%. A more recent simulation, shown in Fig. 1, compares the full-energy peak efficiency for high-energy γ rays in AGATA and in PARIS [1,2]). It it evident that, at 15 MeV, the efficiency of 4π PARIS (which is composed by scintillators 8 inches long) is 4–5 times larger than that of AGATA. Because of the previous points, more than the absolute Full-Energy Peak efficiency

[a] e-mail: franco.camera@mi.infn.it (corresponding author)
[b] e-mail: jisaak@ikp.tu-darmstadt.de
[c] e-mail: adam.maj@ifj.edu.pl
[d] e-mail: sunniva.siem@fys.uio.no

Published online: 25 July 2023

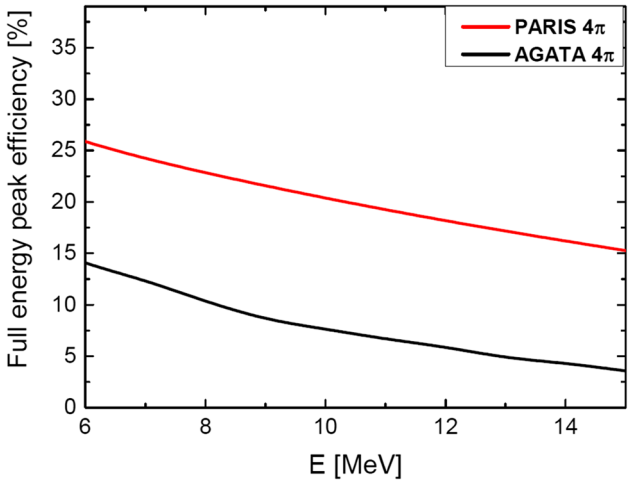

Fig. 1 Calculated efficiency for high-energy γ rays in the range from 6 to 15 MeV of AGATA 4π (namely, 60 triple clusters) and PARIS [1,2] 4π (namely, 150 phoswiches in a minicube geometry) [3]. Note: the values reported in this plots are only indicative, as the real data will depend on adopted geometry and tracking algorithms used

and energy resolution, for experiment involving the detection of high-energy γ radiation, the key factor of AGATA is its unique ability to cleanly select particular reaction channels, shape/deformation, angular momentum, γ multiplicity, coincidence pattern or a very small region of the phase space of the decay paths. This very precise information could be given by the AGATA array and/or by the use of additional ancillary detectors (e.g. detectors for neutrons, for charged particles, mass spectrometers like e.g. PRISMA at LNL and VAMOS at GANIL, etc.).

In the specific case of discrete high-energy γ transitions the possibility to detect them with a resolution of the order of 15–20 keV or less with HPGe detectors allows their identification with better precision than large volume scintillators could do. In fact, the energy resolution of scintillators spreads the counts in a large energy window preventing the identification of discrete transition in the context of experiments devoted to high-energy γ ray measurements. It is also important to use an extremely accurate energy calibration (with a precision of the order of 1 part every ten thousand). In fact, one should overlap few counts measured in different detectors of the AGATA array. Alternatively, one could align the AGATA crystals using a discrete high-energy γ ray from a calibration reaction or from a 'composite' source (for example the AmBeNi or the AmBeFe sources or from the reaction ^{12}C(p,p'γ)^{12}C) producing γ ray with energy in the proximity of the searched γ transition.

The time resolution is instead intrinsically related to the time needed to collect the information carriers. In an AGATA crystal this time is related to the collection of e-h pairs [5]. The typical time resolution of an AGATA crystal is of the order of 15 ns (the time resolution of a fast scintillator like $LaBr_3$:Ce can easily be 1.5 ns or lower). A time resolution of 1 ns implies the inability to localise the γ emissions within a 15 cm sphere radius. A time resolution of 10 ns implies that the sphere has 1.5 m radius. The difference in time of flight (TOF) between a γ ray and a neutron (assuming that the detector is about 20 cm away from the target and assuming a neutron of 4 MeV of kinetic energy) is about 6 ns. To discriminate these neutrons at three standard deviations, a time resolution (FWHM) lower than about 2 ns is required. A time resolution (FWHM) greater than 5 ns makes any kind of neutron discrimination using Time of Flight rather impossible. Tracking, if properly tuned, might help in neutron discrimination as described in reference [6]. Even though very conservative tracking parameters, very accurate GEANT simulations and high statistics are required, tracking could significantly improve the signal to background ratio and partly compensate the not ideal AGATA time resolution [6,7].

Since the excitation energy of a nucleus which emits a high-energy γ ray, could easily be larger than the particle separation energy, high-energy γ rays could be emitted either in alternative or in coincidence with neutrons. In the case of the measurement of high-energy γ rays forming continuous spectra all neutron induced events must be rejected (in the detectors which are expected to measure high-energy γ rays) and thus AGATA, with its time resolution, does not offer this possibility. Conversely, fast scintillators with large volumes provide a 'nanosecond' time resolution (required for effective TOF measurements) or, alternately, detectors characterized by n-γ sensitivity via pulse shape discrimination (e.g. CLYC scintillators [8]) can identify and reject them.

If the TOF technique is used, the scintillators should be located in the forward direction, at least at approximately 20–25 cm from the target. If possible, they should not substitute an AGATA detector but they should be placed in empty spaces. In the case pulse shape discrimination is used, the detectors should be placed very near (some cm) to the target. Also in this case, one should avoid to shadow the AGATA crystals. These general rules must also consider the requirements of the physics case which could provide some specific detector's configurations.

The possibility to improve the time resolution of an HPGe detector has been investigated and a time resolution up to about 3 ns was found (using Pulse shape discrimination algorithms) but this at the cost of rejecting about 90% of the events [9]. This solution cannot be always adopted in a typical nuclear structure experiment searching for rare decays. However, this technique can be employed to reject unwanted events related to possible artefacts, beam halos or beam satellites.

Experiments involving the detection of high-energy γ rays with HPGe detectors were performed in the past. Among them those reported in references [10–13] used (i) a single coaxial HPGe detector, (ii) Euroball Cluster detectors and

(iii) AGATA triple clusters. As expected, the limited size of an HPGe detector strongly affects the absolute 'full-energy peak' efficiency. However, it was possible to increase the relative photopeak efficiency by adding the HPGe energy signals to the energy deposited in the anti-Compton shields [10] or placing more than one HPGe crystals in a single cryostat (as per Euroball [11,12] and the AGATA array [13])

In most of the previous works the calibration and response were deduced using a 15.1 MeV γ ray emitted in the reaction ^{11}B(d,nγ)^{12}C. However it was noted that when the γ multiplicity is equal to one (as in the case of the above reaction) the extracted full-energy peak efficiency is different than that of reactions with γ multiplicity larger than one. In particular, it is expected that the AGATA full-energy peak efficiency (after tracking) for high-energy γ rays strongly depends on the γ multiplicity. In references [14–16] the general performances of the AGATA array are listed.

2 Structure of the Pygmy Dipole Resonance

The investigation of the dipole response of atomic nuclei plays an important role in nuclear physics since many decades, with applications, e.g., in the context of understanding astrophysical objects such as neutron stars and the nucleosynthesis of heavy elements. The observation of substructures in the low-lying electric dipole ($E1$) response located in the excitation-energy region of the low-energy tail of the isovector Giant Dipole Resonance (IVGDR) [17] has triggered a large number of experimental and theoretical studies. The enhanced accumulation of $E1$ strength in the vicinity of the neutron-separation threshold has been observed in many nuclei, and is nowadays often denoted as Pygmy Dipole Resonance (PDR); see Refs. [18–21] for recent reviews. First motivated by considerations within the hydrodynamical model [22] and later also by studies of transition densities in microscopic model calculations (e.g., [21,23,24] and references therein), the PDR is often described macroscopically as an oscillation of an isospin-saturated core against excess neutrons.

Some microscopic models predict a connection between the PDR strength and the neutron-skin thickness (e.g., [25] and references therein) and isovector properties of the equation of state of nuclear matter (see, e.g., [26–30]).

Another consequence of the enhanced $E1$ strength in the PDR region is its role in the synthesis of heavy elements in extreme astrophysical environments such as neutron stars and in the recently observed neutron-star merger event [31], that showed to be a well-suited location for r-process reactions. Due to its location in the vicinity of the neutron-separation threshold, the PDR has an impact on predictions of the nucleosynthesis in the r-process [32] and in neutron capture reaction rates [33–37] in astrophysical network calculations. Despite all the experimental and theoretical efforts in the past years, the interpretation of the PDR as a collective neutron-skin oscillation is still under debate. Other interpretations such as a toroidal nature that is linked to a confined vortical flow within the nucleus [38,39] and a dominant single-particle structure assigned to most of the PDR states [40,41] are currently discussed.

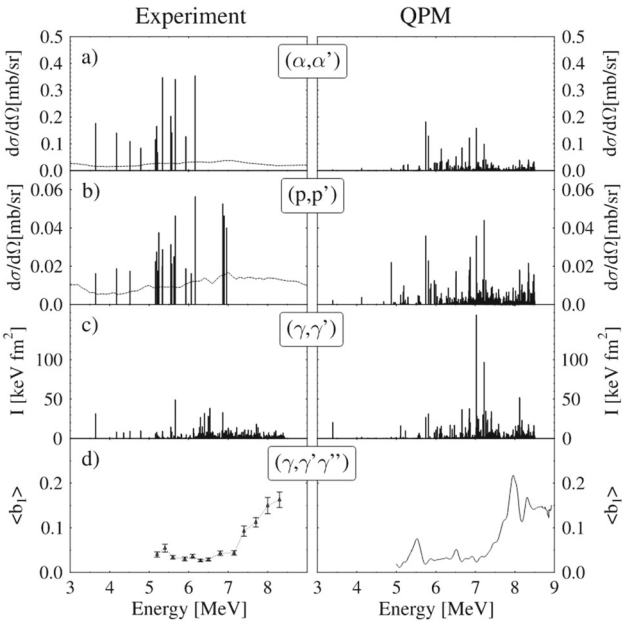

Fig. 2 Comparison of experimental and theoretical results for the structure of the PDR of ^{140}Ce from four different complementary reactions. Reprinted from Ref. [44]. Figure is licensed under a Creative Commons Attribution 4.0 license

To date, most studies of the low-energy electric dipole strength were performed on stable nuclei using isovector probes such as real [42] and virtual photons [20,43]. However, for an in depth investigation of the microscopic structure and the nature of the PDR, extensive studies using different reaction channels and complementary probes are crucial.

One milestone in the investigation of the PDR are experiments with isoscalar hadronic probes like α particles and ^{17}O ions. A structural splitting of the low-lying $E1$ strength in numerous nuclei was observed in (α, α' γ) [45–47] and (^{17}O, $^{17}O'$ γ) [19,48,49] reactions using either single-crystal HPGe or the highly-segmented tracking detector array AGATA for the coincident γ ray detection. A prominent example is shown in Fig. 3 for the case of ^{124}Sn from Ref. [48]. The ^{17}O-scattering experiments benefited from the excellent energy resolution and photopeak-to-total detection efficiency of AGATA in the particle-γ coincidence measurements.

The combination of various complementary datasets has opened the possibility to detailed investigations of the PDR in comparison to nuclear models [21,44]. Figure 2 illustrates such "multi-messenger investigation" comparing measured

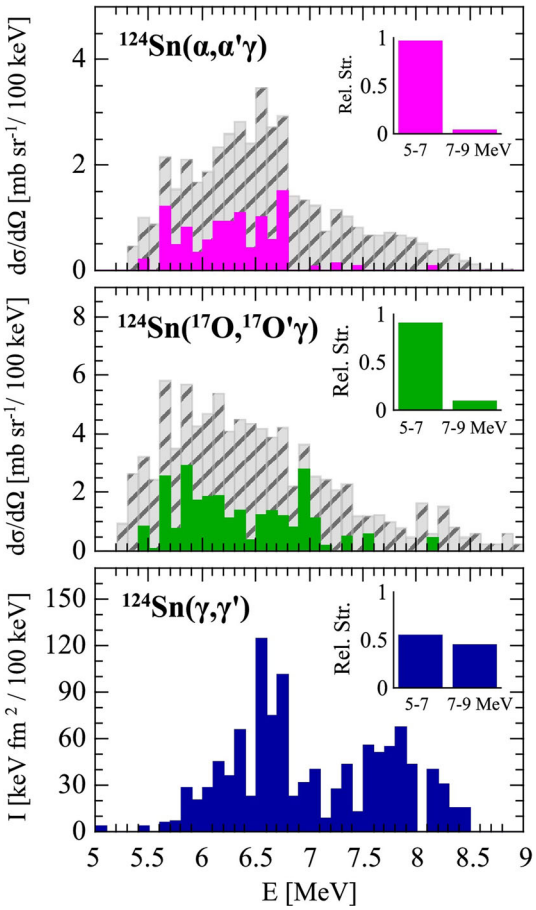

Fig. 3 Measured differential cross section in ^{124}Sn($^{17}O, ^{17}O'\gamma$) reactions using AGATA as γ spectrometer in comparison to data from ($\alpha, \alpha'\gamma$) and (γ, γ') experiments. Reprinted from Ref. [48]. Figure is licensed under a Creative Commons Attribution 4.0 license

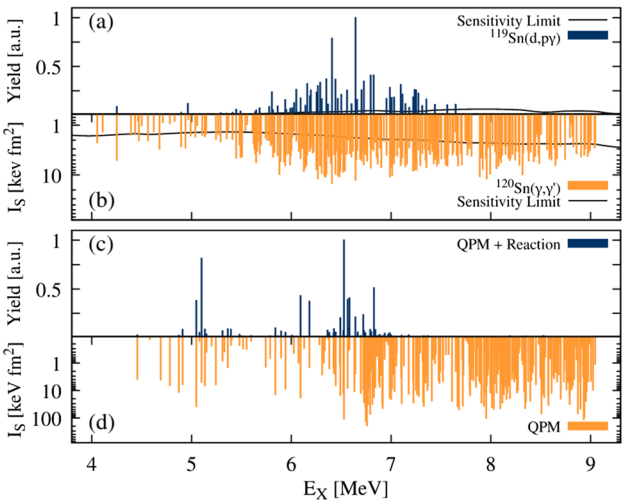

Fig. 4 **a** Relative γ-ray yields from ^{119}Sn(d,pγ) and **b** en- energy-integrated cross sections I_S for ^{120}Sn(γ, γ') reactions. The corresponding theoretical results are displayed in (**c**) and (**d**). Reprinted with permission from Ref. [41]. Copyright (2022) by the American Physical Society

reaction cross sections and average branching ratios of PDR states in ^{140}Ce obtained from α, proton, and real-photon scattering experiments [44] with corresponding calculations in the quasiparticle phonon model (QPM) within a semiclassical approximation [121].

So far scarce information on the one-particle-one-hole (1p-1h) and two-particle-two-hole (2p-2h) components contributing to the overall structure of the PDR is available. Hence, β-decay reactions populating PDR states and the subsequent observation of their γ decay were added to the collection of experimental observables [50,51] enabling the study of 1p-1h or more complex configurations. In this regard, nucleon-transfer reactions are excellent for studying the single-particle structure of the PDR. Very recent (d,p) [40] and (d,pγ) [41] reactions were utilised to explore the 1p-1h contributions to individual 1^- states of ^{208}Pb and ^{120}Sn, respectively. In particular, the ^{119}Sn(d,pγ) nucleon-transfer reaction study highlights the importance for a consistent treatment of nuclear structure and reaction theory to test the wave functions of potential PDR states illustrated in Fig. 4 and discussed in Ref. [41].

Neutron 1p-1h components of potential doorway states may influence contributions from neutron and γ channels of neutron-capture reactions [52]. Furthermore, the detailed structure of PDR states may strongly impact (n,γ) cross sections and consequently isotope production in explosive stellar environments, see, e.g., Refs. [34,53]. In this view, it is of great importance to extend the experimental and theoretical studies of the structure of the PDR with complementary probes as done for stable nuclei and for unstable neutron-rich isotopes. These studies will provide stringent tests of state-of-the-art nuclear structure theory and allow to further develop the modeling of neutron-capture reactions in exotic nuclei which play a crucial role in the nucleosynthesis as for example in the r process.

As discussed above, one of the key methods to identify 1^- states in a multitude of nuclear states with different spin and parity quantum numbers, is the selection of the ground-state γ decay following the nuclear excitation. It is noted, that experiments with exotic neutron-rich nuclei imply reactions in inverse kinematics. Because the γ rays are emitted in-flight from the excited projectiles, a high-resolution tracking detection array paired with a superb photopeak-to-total detection efficiency is key to perform the Doppler corrections of the observed γ rays. These demanding requirements make AGATA the detector array of choice for future experiments with respect to revealing the structure of the PDR in unstable neutron-rich nuclei.

Potential complementary investigations of the PDR in exotic isotopes include experiments with virtual photons and

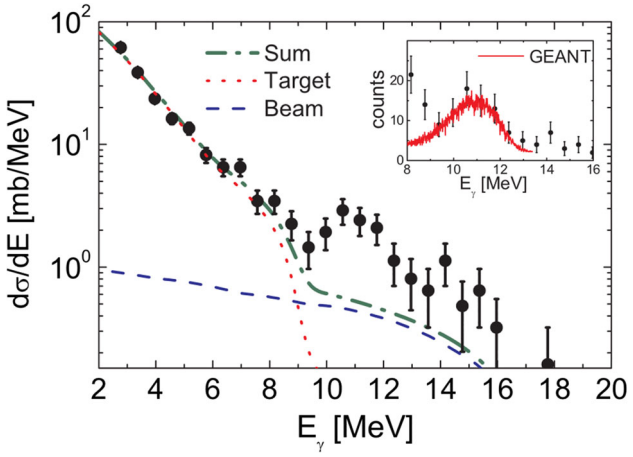

Fig. 5 The high-energy γ-ray spectrum measured with BaF_2 detectors. The lines indicate the statistical model calculations for the target emission (dotted line) and the beam emission not considering the PDR (dashed line) and their sum (dot dashed line). Inset: GEANT simulation for a γ transition at 11 MeV. The measured width is due to both the energy resolution of the BaF_2 detector and the Doppler broadening effect. Reprinted with permission from Ref. [54]. Copyright (2022) by the American Physical Society

nucleon-transfer reactions in the Ni-Zn and the Sn region. This will allow for a thorough testing of nuclear structure and reaction theories via the study of the evolution of the PDR along the Ni, Zn, and Sn isotopic chains from stable to unstable isotopes with a large variation of the neutron-to-proton ratio. The virtual photon-scattering technique using the RISING setup at the fragment separator of GSI successfully demonstrated the possibility to observe the PDR in ^{68}Ni [54]. Figure 5 displays the corresponding measured γ-ray spectrum using ^{68}Ni as incident beam.

Similar measurements with AGATA will provide promising opportunities for further studies of the PDR in the Ni-Zn region at GSI/FAIR. Hence, it will allow extending the nucleon-transfer reaction studies along the Ni and Sn isotopic chains such as from ^{120}Sn [41] towards ^{132}Sn.

Possible setups to detect light ejectiles from nucleon-transfer reactions are MUGAST [55] or in the future GRIT [56], which is currently under development and in the test phase (see e.g. [57]). Coupling the detection system for heavy ions GRIT [56] to AGATA will allow for the coincident detection of γ rays emitted in-flight. A coincident measurement of both quantities, E_x with GRIT and E_γ with AGATA, will allow for the selection of ground-state γ-ray decays and thus predominantly 1^- states in the corresponding reactions. The GRIT-AGATA setup will open the possibility to extend the study of the single-particle structure of the PDR from stable to neutron-rich unstable nuclei via (d,pγ) and (p,dγ) reactions in inverse kinematics, for instance at SPES [58] and GSI/FAIR [59], which will produce exotic ion beams with high beam intensities. GRIT-AGATA@SPES and GRIT-AGATA@FAIR will be a promising combination to extend studies of the PDR to so far unreached regions on the nuclear chart and extract novel information on the structure of low-energy $E1$ excited states and their impact on the nucleo-synthesis of heavy elements beyond the Fe mass region.

3 Nuclear level density and photon strength functions using the Oslo method

High-energy gamma rays measured with AGATA can also be used to extract the nuclear level density (NLD) and photon strength function (PSF), using the Oslo Method [60,61]. The Oslo method is a technique which allows for the simultaneous extraction of nuclear level density and photon strength function from charged-particle-γ coincidences data. This method probes the PSF below the neutron separation energy. One important step of the method is to obtain the distribution of primary γ rays (the first-emitted γ rays in all decay cascades), which contains information on the NLD and PSF.

Until recently, the experiments have been performed at the Oslo Cyclotron Laboratory (OCL), which has an optimised experimental setup for measuring light-ion induced reactions. The outgoing charged particles are measured with the Silicon Ring (SiRi) detector array and the emitted γ rays were measured with the CACTUS array [62] and more recently the upgraded OSCAR array [63], consisting of 30 large volume $LaBr_3$:Ce detectors. It would be very interesting to perform similar experiments with AGATA, as the excellent energy resolution and granularity of AGATA offers a great advantage over the scintillator detectors, and we would expect a much higher energy resolution for the photon strength function results.

The pygmy dipole resonance described in detail in the previous section, has also been observed in all the Sn isotopes [64,65] measured using the Oslo method. This method measures the total strength function and cannot distinguish between E1 and M1, so it is assumed that the extra strength on the tail of the GDR is E1 being in the energy range of the pygmy resonance described in the previous section.

The NLD and PSF are key ingredients in Hauser-Feshbach theory [66,67] to calculate nuclear reaction rates, for example using TALYS [68]. This has recently been done for the ^{191}Os(n,γ) [69] and ^{126}Sb(n,γ) [70] reactions. By measuring the NLD and PSF in charged-particle induced reactions, it is possible to constrain calculations of neutron-capture reaction rates in cases where direct (n,γ) measurements are not feasible.

An increased strength at around 3 MeV, interpreted as the scissors resonance, has also been observed in several rare earth nuclei [71–73], and in several actinide nuclei with much larger strength than in the rare earth nuclei. Experiments on

various Th, U, Np, and Pu targets yielded systematic studies of level densities [74,75], the strength of the scissors resonance [76–79], and the validity of the Brink-Axel hypothesis [65,80]. Neutron capture cross section from evaluated data libraries like the TENDL [81], JENDL-5 [82] and JEFF−3.3 [83], usually agree well with direct (n,γ) measurements up to neutron energies of 200 keV, where data are available. However, predictions for cross sections at higher neutron energies differ significantly depending on the models used for the PSF. Using the measured NLD and PSF as inputs in TALYS [68] it is possible to constrain the neutron capture rates for neutron energies from 200 keV to several MeV.

A low-energy enhancement of the PSF has been observed first in Iron isotopes [84] and since then in many other nuclei across the nuclear chart. From angular correlations measurements it was shown to be of dipole character [85]. As already pointed out, the results from the Oslo method are not able to differentiate between the M1 and E1 components. However, shell model calculations predicts the low-energy enhancement to be M1 [86]. The low-energy enhancement in all the measured molybdenum isotopes [87] seem to follow the same energy trend. By assuming that the same energy trend continues towards neutron rich nuclei, the effect on the neutron capture rates becomes important [88]. This effect motivated experiments to measure the PSF in more neutron-rich nuclei. The inverse-kinematics- and beta-Oslo methods [89,90] are variants of the Oslo method developed specifically for exotic nuclei, which will enable us to provide new data for nucleosynthesis processes involving neutron-rich nuclei. Again with the excellent energy resolution and high granularity of AGATA, this detector array would be ideal to apply the Oslo Method in inverse kinematics experiments. Especially the high granularity gives a great advantage over large scintillator detectors when it comes to perform Doppler corrections to the γ-energies. To detect the outgoing charged particle AGATA would need to be coupled to MUGAST [55] or in the future GRIT [56] as already discussed in the previous section.

The main systematic uncertainty of the Oslo method is related to model assumptions about the spin dependence of the NLD [91]. This uncertainty also affects the PSF and neutron capture cross sections extracted from the data. The excellent energy resolution of AGATA, with the possibility to measure resolved particle-γ-γ coincidences, offers an unique opportunities to investigate the spin dependence of the NLD.

Gating on discrete transitions along the yrast line the statistical γ rays originating from states of different spin ranges will be selected, and the energy of the ejectile will provide the excitation energy of the initial state. It is therefore possible to generate subsets of data corresponding to different spin ranges, which will be analyzed separately using the Oslo method, disentangling the spin dependence of the NLD and PSF. The results will be used to validate and improve level density models, to reduce systematic uncertainties of the Oslo method, and to improve the predictive power of cross section calculations based on experimental NLD and PSF obtained using the Oslo method. AGATA could also be used in experiments using heavy-ion beams, which transfer more angular momentum, and which would yield to the total level density without limitations in spin imposed by light-ion reactions.

Experiments using the Oslo method have so far been limited to excitation energies below the neutron separation energy. The excellent energy resolution of AGATA makes it possible to study the competition between neutron and γ emission above the neutron threshold by analyzing coincidences with energy-resolved discrete transitions in the nucleus of interest. Such measurements will provide direct and quantitative information about the competition between γ and neutron decay, which is highly important input for reaction network calculations of nucleo-synthesis in stellar environments. In addition, in favorable cases it might be possible to extend the studies of the NLD and PSF beyond the neutron separation energy. This would be an important achievement, because it would allow to connect the PSF obtained with the Oslo method with those obtained from (γ,n) measurements. Such a comparison would yield much more reliable results for pygmy resonances located in the region of the neutron separation energy.

4 Ground state and low-lying states decay of gaint resonances

Giant Resonances (GR), collective modes of excitation in the atomic nucleus have been extensively investigated for many years, giving an exclusive look into the bulk properties of this system. Their properties can be, for example, linked to basic parameters of the nuclear equation of state (EoS) (cf. [92]). Especially, the measurement of the γ decay of the isovector giant dipole resonance (IVGDR) has proved to be a powerful tool to access information about the angular momentum and temperature evolution of the shape of the excited nucleus [93]. It has been predicted recently [94], that the comparison of the direct γ decay width to low-lying states (first 2^+ in the case of IVGDR and first 3^- - for isoscalar giant quadrupole resonance ISGQR) is a unique probe of the resonance wave function, and a testing ground for nuclear structure models. In addition, there were predictions showing that γ decay of the isoscalar giant quadrupole resonance (ISGQR) should also be sensitive to the deformation [95]. However, a more detailed understanding of the wave functions of the GRs, as well as their decay properties is still far from being satisfactory. And this is because so far only two measurements of ISGQR gamma decay, and only to the ground state, have been reported [96,97] for ^{208}Pb. The rea-

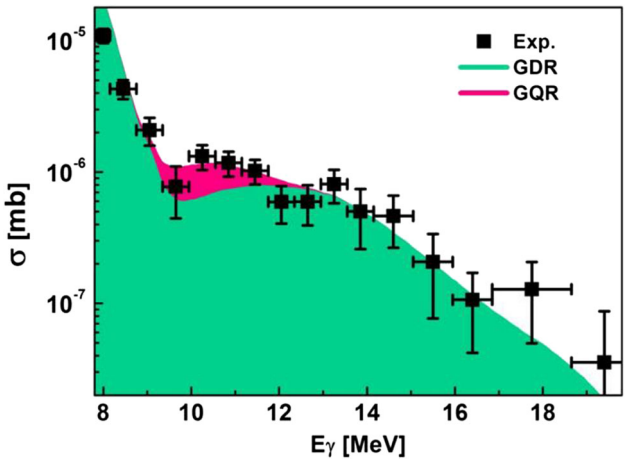

Fig. 6 Cross-section for the gamma photons emitted to the ground state by ^{208}Pb excited by protons. The existence of oscillations caused by the GQR is evidenced by the area marked in red on top of the IVGDR spectrum (green). Copyright (2022) by Institute of Nuclear Physics PAN

son for the lack of the experimental data is the difficulty of the measurement: the γ decay above the neutron threshold (in the case of ^{208}Pb S_n = 7.368 MeV) is hindered by the competing channel of neutron emission, and because the branching ratio for the gamma decay of GQR is at least two orders of magnitude smaller than the gamma decay of GDR (see Fig. 6). This makes a problem of disentangling the contributions of the two decays to the gamma-ray spectrum. So far this was done by fitting the known GDR response to the part of the spectrum which was expected to be free from the ISGQR decay and by subtracting such a fit from the total spectrum. One could expect that by coupling a modular germanium array like AGATA and a high-energy detector (for example by coupling AGATA to the PARIS scintillator array [1,2]) a certain experimental progress can be achieved. First of all those two types of gamma-decay (from IVGDR and from ISGQR) are expected to have different angular distributions: mainly dipole for IVGDR and mainly quadrupole for ISGQR. Therefore by measuring the angular distributions of the gammas in respect to the beam direction, and by adopting a multipole decomposition analysis of the angular distributions (e.g. [98]) to the gamma spectrum, one will be able to better distinguish between the IVGDR and ISGQR contributions to the high-energy gamma spectrum. Moreover, using AGATA and PARIS, one will be able to select the GR gamma decays to specific discrete structures (2^+, 3^-), what gives the possibility to measure the widths the decay of the GRs to low-lying vibrational states. This in turn provides an effective approach to access directly the microscopic structure of the Giant Resonances.

5 IVGDR on extreme shapes

If it is needed, in the same detector, to totally reject neutron induced events by TOF technique and to measure the high-energy γ ray spectrum, it is necessary to couple AGATA with an array of fast and efficient detectors (for example large volume scintillators).

In this type of measurements, an apparatus such as AGATA is certainly able to select specific nuclear configurations leaving the measurement of high-energy γ rays and the rejection of neutron induced events to other fast and efficient type of detectors. For example, by coupling AGATA with a large volume scintillator array (e.g. PARIS), it will be possible to measure the γ decay of the Isovector Giant Dipole Resonance (IVGDR) in coincidence with (i) specific regions of the phase space (that correspond to specific shapes or orientations of the nucleus), (ii) super-deformed bands or (iii) specific low lying transitions associated to particular shapes, deformations or angular momentum.

In the case of the IVGDR built on a compound nucleus produced through a fusion-evaporation reaction, the branching ratio of the IVGDR decay for the emission of γ radiation at 8 MeV with respect to the emission of one neutron of any energy is of the order of 10^{-3}. For this type of measurements, one needs a very efficient experimental apparatuses for the detection of both high-energy γ rays and discrete low-energy γ radiation. In addition, the setup should be capable to totally reject the contribution of neutrons induced events. A quantitative estimation of the probability to measure, in coincidence, a 1 MeV γ ray in one AGATA cluster and a 15 MeV γ ray in a PARIS cluster is about 0.2%.

Recently, an experiment was carried out at the ALTO accelerator of IJCLab where the ^{192}Pt compound nucleus was created using the reaction ^{18}O + ^{174}Yb with E_{beam} = 82 MeV (see Fig. 7 for a preliminary spectrum). After the evaporation of 4 neutrons ^{188}Pt is populated [99]. If ^{192}Pt evaporates five neutrons (populating ^{187}Pt) no energy is left for the γ decay of the IVGDR as Fig. 7 shows. The nucleus ^{188}Pt presents an axial deformation coexisting with a quasi-prolate one [100].

The coincident measurement of high-energy γ rays with discrete transitions will provide information about the shape and deformation of the 'hot-nucleus' which fed that particular transition. If different structures of ^{188}Pt are in coincidence with different high-energy γ ray spectra, there is a clear evidence of a preferred decay-path to feed specific shapes or deformations in the residue nucleus. In this case it will be possible to isolate a 'particular' shape or deformation by the selection of preferential decay path.

Reference [101] reports a measurement in which the IVGDR γ decay is in coincidence with a high spin isomeric transition in ^{216}Rn. This condition fix the minimum angular momentum that the nucleus must have and, therefore, con-

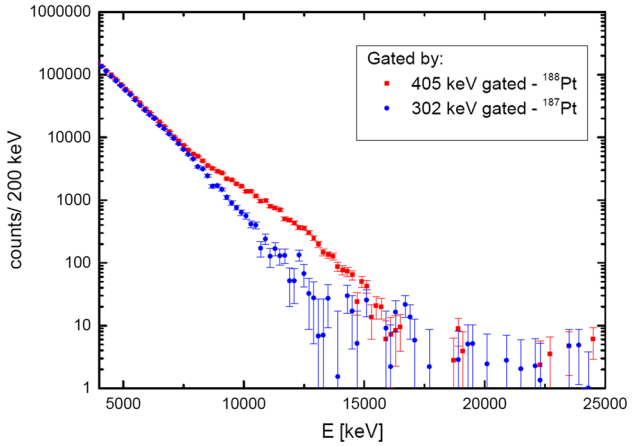

Fig. 7 The GDR gated on 4n channel ^{188}Pt (filled red points) and 5n channel ^{187}Pt (filled blue points) [3]. The blue points have been obtained selecting the high-energy gamma rays in coincidence with the 302 keV line in ^{187}Pt while the red points are in coincidence with the 405 keV line in ^{188}Pt [3]

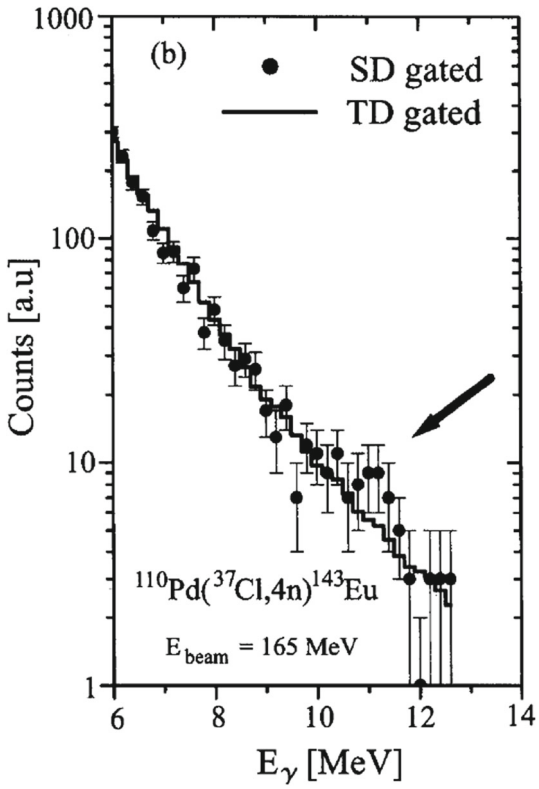

Fig. 8 GDR gated on SD discrete transitions; the figure was taken from reference [108] The figure is reproduced with permission from [108], © 2001, by Elsevier

tains a specific small region of the phase space at high angular momentum.

Some years ago, a challenging measurement to search for the IVGDR built on super-deformed (SD) structures in ^{143}Eu was made (using HPGe detectors) [102–104]. In that measurement the compound nucleus ^{147}Eu, leading to the residue ^{143}Eu at high spin was populated through the fusion-evaporation reaction ^{110}Pd + ^{37}Cl with beam energy of 165 MeV. The experiment was performed first at the TANDEM laboratory in Risoe (using NORDBALL and the HECTOR array [105,106]) and then, the same reaction was repeated at the INFN National Laboratories of Legnaro using EUROBALL and HECTOR [106,107]. Although the most efficient apparatuses of the time had been used, the statistics collected was not enough [19,108] to draw firm conclusions (see Figs. 8 and 9) on the evidence of the dipole oscillation built on super-deformed configurations. This coupling is interesting also because this mechanism was invoked to justify the intensity of the super-deformed bands.

At the moment, the question of the population of the super-deformed bands appears to be a problem needing further investigation based on experiments with higher detection efficiency and selectivity. Future experiments should have the ambition to address the question on whether or not there is a preferential path for the population of these structures. The preferential path is due to the component of the IVGDR centered at around 10 MeV (30% of the total IVGDR strength) characterizing the dipole oscillation along the super-deformed axis,

In Fig. 1 of [109] it is shown with very simple arguments that the transition probability of E1 statistical decay (hence the gamma decay of the IVGDR) is about ten times greater in the case of a highly deformed system. This increase in transition probability is due to the different density of levels present in a super-deformed system compared to a system normally deformed and to the fact that, since the IVGDR is coupled to the nuclear deformation, the oscillation along the major axis of a nucleus corresponds to the emission of γ rays of about 10 MeV while in the normally deformed case γ rays of 13–15 MeV are expected.

In addition, one could also deduce if a super-deformed system has [109] a lower-level density as compared with normal deformed states.

To address (and hopefully solve) the problem of the population of the super-deformed bands, experiments for a variety of nuclei and using arrays such as AGATA [14–16,110] and PARIS [1,2] should be performed. The PARIS cluster has about the same efficiency as 1.5 detectors of the HECTOR array [106] and, assuming to have 12 PARIS clusters, the increase in efficiency would be about a factor of 2 larger than that of HECTOR [106] used in the past.

For the detection of low-energy transition from super-deformed bands, to be measured in coincidence with high-energy γ rays, the gain factor, as compared with old experiments, is due to the increase of both the solid angle subtended by all the AGATA clusters (3/4 of the whole solid angle is covered) and of the acquisition rate. This will results

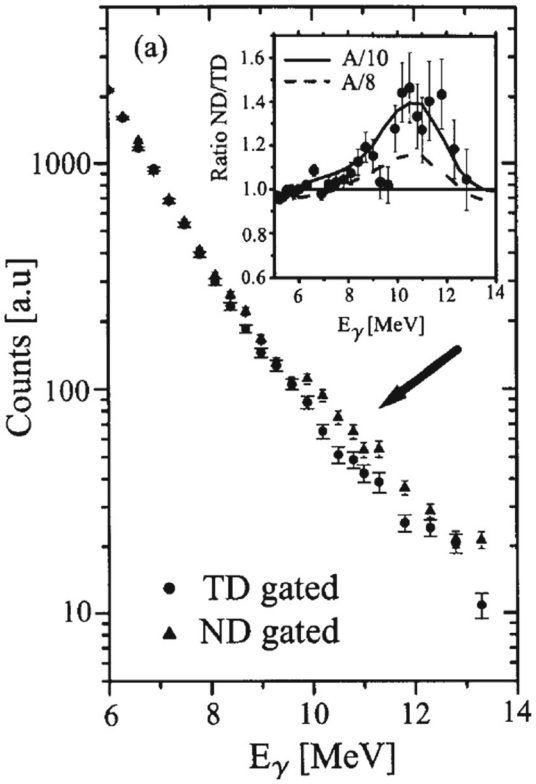

Fig. 9 The GDR gated on TD and ND discrete transitions; the figure was taken from reference [108] The figure is reproduced with permission from [108], © 2001, by Elsevier

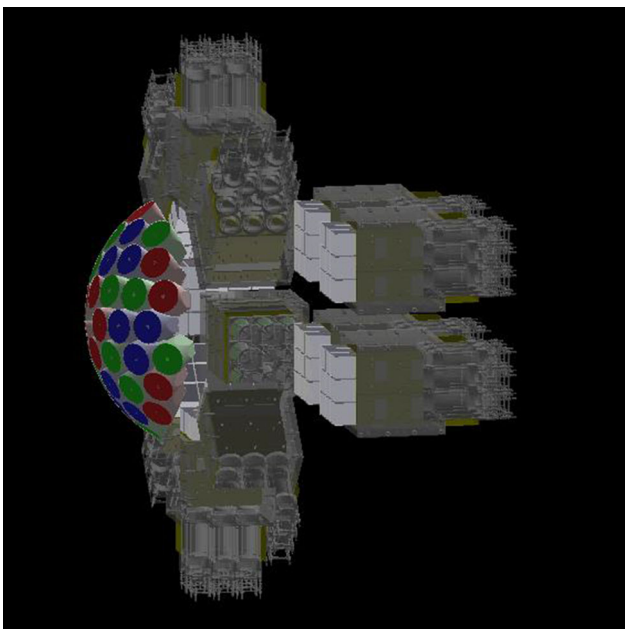

Fig. 10 An example of coupling geometry of AGATA and the PARIS array. As discussed in the text, the scintillators are placed in a forward direction while HPGe are placed backwords

in a spectrum with statistics at least 20–40 times higher than the one reported in reference [108] and thus the error bars in spectra as those in Fig. 8 will be reduced at least by a factor of 4–5). This estimate was extracted using the data reported in reference [3,16,110]. With this reduced error a better understanding of the population of the SD structures can be achieved.

The Fig. 10 shows an example of how one can couple a scintillator array like PARIS [1,2] to AGATA. As was done with NORDBALL [105] and EUROBALL [107] in the past, one must design a geometry which firstly should depend on the physics case but that should also minimize the number of removed detectors. In addition, one preferably should place HPGe crystals in the backward angles to avoid possible neutron damage. In fact, in general, scintillators are more resistant to neutron damage than solid state detectors.

Another interesting phenomenon that can also be studied by coupling AGATA array to a highly efficient fast scintillator arrays (as for example PARIS) is the so-called Jacobi shape transition: an abrupt change of the nuclear shape at the highest spins from an oblate non-collectively rotating ellipsoid via triaxial shapes to elongated collectively rotating prolate elipsoid [111,112]. Such a phenomenon is evidenced in the Giant Dipole Resonance strength function as large splitting of the Lorentzian shape, with a low energy component whose centroid energy is close or below the particle threshold. Such phenomenon was already observed in a number of light nuclei (around A = 45) [113–116], but it is expected to be even more pronounced in medium mass nuclei. It was also observed that this low energy component is correlated with the cold structures of high deformations [117]. Therefore, it was speculated that the extreme deformations of hot compound nuclei might be preserved during the evaporation process, so that the Jacobi shapes might be a gateway to the super- or hyper-deformations [118]. This hypothesis is however still lacking a direct experimental proof [119].

An additional phenomenon, similar to the one previously mentioned, predicted by theory, and not yet experimentally verified, is the so-called Poincare shape transition [120]. At a certain critical value of angular momentum, the system loses stability against the left-right symmetry, and becomes pear-shaped (or octupole). Such deformation shall result in even more fragmented IVGDR strength, with components of low energies, much below the particle threshold.

6 Conclusions

The investigation of high-energy γ radiation emitted by excited nuclei during their decay towards the ground state provides unique nuclear structure explorations and leads to a wealth of important information to test nuclear models. High-energy γ rays have different origins. One origin could

be the decay of a discrete state (see for example the 15.1 MeV 1^+ state in ^{12}C) generally located in the continuum or in proximity of the particle binding energy. Another one is the electromagnetic decay of dipole states either based on ground state or on excited state as the compound nucleus (like for example the IVGDR). Since the excitation energy involved is in many cases larger than the particle separation energy, the high-energy γ rays are frequently in competition and/or in coincidence with charged particles or neutron radiation.

The very high granularity of AGATA, its superior energy resolution together with the possibility to be coupled with ancillary detectors, allow selective measurements as those requiring the investigation of small regions of the phase space. Experiments on the interesting open problems here discussed, requiring high-energy γ ray detection will benefit on the increasing number of AGATA detectors. The planning of the future program here presented will take this into account, together with the aim to progress considerably on these appealing topics.

Acknowledgements The authors want to thank the AGATA collaboration and in particular A. Bracco, M. Ciemala, F.C.L. Crespi, M. Kmiecik, S. Leoni, B. Million, O. Wieland. J. I. acknowledges the support by the State of Hesse under grant "Nuclear Photonics" within in the LOEWE program and within the Research Cluster ELEMENTS (Project ID 500/10.006), and support from the Research Council of Norway grant "Nuclear shapes and resonances" (grant no. 325714). We acknowlegde the laboratories, where the experiments leading to the results presented in this paper were achieved: GSI Darmstadt, OCL Oslo, NBI Copehnagen, IPHC Strasbourg, CCB IFJ PAN Kraków, IJCLab Orsay, LNL Legnaro.

Funding Open access funding provided by Università degli Studi di Milano within the CRUI-CARE Agreement.

Data Availability Statement This manuscript has no associated data or the data will not be deposited. [Authors' comment: It is a review paper and therefore there is not a specific dataset which was analyzed.]

References

1. A. Maj et al., Acta Phys. Pol. B **40**, 565 (2009)
2. F. Camera and A. Maj, "PARIS White Book". http://rifj.ifj.edu.pl/handle/item/333
3. M. Ciemala private communications
4. I.Y. Lee, M.A. Delaplanque, K. Vetter, Developments in large gamma-ray detector arrays. Rep. Prog. Phys. **66**, 1095 (2003). https://doi.org/10.1088/0034-4885/66/7/201
5. G. Knoll, Radiation Detection and Measurement. John Wiley and Son Inc
6. M. Senyigit et al., Identification and rejection of scattered neutrons in AGATA. Nucl. Inst. Method Phys. Res. Sect. A: Accel. Spect. Det. Ass. Equip. **735**, 267 (2014) https://doi.org/10.1016/j.nima.2013.09.035
7. R. Avigo et al., Low-lying electric dipole γ-continuum for the unstable ^{62,64}Fe nuclei: strength evolution with neutron number. Phys. Lett. B **811**, 135951 (2020). https://doi.org/10.1016/j.physletb.2020.135951
8. https://www.rmdinc.com/
9. F.C.L. Crespi et al., HPGe detectors timing using pulse shape analysis techniques. Nucl. Inst. Meth. Phys. Res Sect.: A Accel. Spect. Det. Ass. Equip. **620**, 299 (2010) https://doi.org/10.1016/j.nima.2010.02.273 (**and references therein**)
10. F. Camera et al., The response of a HPGe detector with a BGO shield to high energy γ-rays. Nucl. Inst. Method Phys. Res. Sect. A: Accel. Spect. Det. Ass. Equip. **351** ,401 (1994) https://doi.org/10.1016/0168-9002(94)91369-2 (**and references therein**)
11. M. Wilhelm et al., The response of the Euroball Cluster detector to γ-radiation up to 10 MeV. Nucl. Inst. Method Phys. Res Sect. A: Accel. Spect. Det. Ass. Equip. **381**, 462 (1996) https://doi.org/10.1016/S0168-9002(96)00793-0
12. B. Million et al., Measurement of 15 MeV [gamma]-rays with the Ge cluster detectors of EUROBALL. Nucl. Inst. Method Phys. Res. Sect. A: Accel. Spect. Det. Ass. Equip. **452**, 422 (2000). https://doi.org/10.1016/S0168-9002(00)00444-7 (**and references therein**)
13. F.C.L. Crespi et al., Response of AGATA segmented HPGe detectors to gamma rays up to 15.1 MeV Nucl. Inst. Method Phys. Res Sect. A: Accel. Spect. Det. Ass. Equip. **705**, 47 (2013). https://doi.org/10.1016/j.nima.2012.12.084 (**and references therein**)
14. S. Akkoyun et al., AGATA-advanced GAmma tracking array. Nucl. Inst. Method Phys. Res. Sect. A: Accel. Spect. Det. Ass. Equip **668**, 26 (2012). https://doi.org/10.1016/j.nima.2011.11.081
15. E. Clements et al., Conceptual design of the AGATA array at GANIL. Nucl. Inst. Method Phys. Res Sect. A: Accel. Spect. Det. Ass. Equip **855**, 1 (2017). https://doi.org/10.1016/j.nima.2017.02.063
16. W. Koerten et al., Physics opportunities with the Advanced Gamma Tracking Array: AGATA. Eur. Phys. J. A (2020). https://doi.org/10.1140/epja/s10050-020-00132-w
17. M.N. Harakeh, A. van der Woude, *Giant Resonances* (Oxford University Press, 2001)
18. D. Savran, T. Aumann, A. Zilges, Experimental studies of the Pygmy Dipole Resonance. Prog. Part. Nucl. Phys. **70**, 210 (2013). https://doi.org/10.1016/j.ppnp.2013.02.003
19. A. Bracco, F.C.L. Crespi, E.G. Lanza, Gamma decay of pygmy states from inelastic scattering of ions. Eur. Phys. J. A **51**, 99 (2015). https://doi.org/10.1140/epja/i2015-15099-6
20. A. Bracco, E.G. Lanza, A. Tamii, Isoscalar and isovector dipole excitations: nuclear properties from low-lying states and from the isovector giant dipole resonance. Prog. Part. Nucl. Phys. **106**, 360 (2019). https://doi.org/10.1016/j.ppnp.2019.02.001
21. E.G. Lanza, L. Pellegri, A. Vitturi, M.V. Andres, Theoretical studies of Pygmy Resonances. Prog. Part. Nucl. Phys. **129**, 104006 (2023). https://doi.org/10.1016/j.ppnp.2022.104006
22. R. Mohan, M. Danos, L.C. Biedenharn, Three-fluid hydrodynamical model of nuclei. Phys. Rev. C **3**, 1740 (1971). https://doi.org/10.1103/PhysRevC.3.1740

23. E. Litvinova, P. Ring, V. Tselyaev, Relativistic quasiparticle time blocking approximation: dipole response of open-shell nuclei. Phys. Rev. C **78**, 014312 (2008). https://doi.org/10.1103/PhysRevC.78.014312
24. E.G. Lanza, A. Vitturi, M.V. Andres, F. Catara, D. Gambacurta, Excitations of pygmy dipole resonances in exotic and stable nuclei via Coulomb and nuclear fields. Phys. Rev. C **84**, 064602 (2011). https://doi.org/10.1103/PhysRevC.84.064602
25. E. Litvinova, P. Ring, V. Tselyaev, K. Langanke, Relativistic quasiparticle time blocking approximation. II. Pygmy dipole resonance in neutron-rich nuclei. Phys. Rev. C **79**, 054312 (2009). https://doi.org/10.1103/PhysRevC.79.054312
26. J. Piekarewicz, Pygmy dipole resonance as a constraint on the neutron skin of heavy nuclei. Phys. Rev. C **73**, 044325 (2006). https://doi.org/10.1103/PhysRevC.73.044325
27. A. Carbone et al., Constraints on the symmetry energy and neutron skins from pygmy resonances in ^{68}Ni and ^{132}Sn. Phys. Rev. C **81**, 041301 (2010). https://doi.org/10.1103/PhysRevC.81.041301
28. X. Roca-Maza, G. Pozzi, M. Brenna, K. Mizuyama, G. Colò, Low-lying dipole response: Isospin character and collectivity in ^{68}Ni, ^{132}Sn, and ^{208}Pb. Phys. Rev. C **85**, 024601 (2012). https://doi.org/10.1103/PhysRevC.85.024601
29. P. Papakonstantinou, H. Hergert, R. Roth, Isoscalar and neutron modes in the $E1$ spectra of Ni isotopes and the relevance of shell effects and the continuum. Phys. Rev. C **92**, 034311 (2015). https://doi.org/10.1103/PhysRevC.92.034311
30. Z.Z. Li, Y.F. Niu, W.H. Long, Electric dipole polarizability in neutron-rich Sn isotopes as a probe of nuclear isovector properties. Phys. Rev. C **103**, 064301 (2021). https://doi.org/10.1103/PhysRevC.103.064301
31. B.P. Abbott et al., Multi-messenger observations of a binary neutron star merger. Astrophys. J. Lett. **848**, L12 (2017). https://doi.org/10.3847/2041-8213/aa91c9
32. S. Goriely, Radiative neutron captures by neutron-rich nuclei and the r-process nucleosynthesis. Phys. Lett. B **436**, 10 (1998). https://doi.org/10.1016/S0370-2693(98)00907-1
33. H. Utsunomiya et al., γ-ray strength function for ^{116,117}Sn with the pygmy dipole resonance balanced in the photoneutron and neutron capture channels. Phys. Rev. C **80**, 055806 (2009). https://doi.org/10.1103/PhysRevC.80.055806
34. E. Litvinova et al., Low-lying dipole response in the relativistic quasiparticle time blocking approximation and its influence on neutron capture cross sections. Nucl. Phys. A **823**, 26 (2009). https://doi.org/10.1016/j.nuclphysa.2009.03.009
35. I. Daoutidis, S. Goriely, Large-scale continuum random-phase approximation predictions of dipole strength for astrophysical applications. Phys. Rev. C **86**, 034328 (2012). https://doi.org/10.1103/PhysRevC.86.034328
36. N. Tsoneva, S. Goriely, H. Lenske, R. Schwengner, Pygmy resonances and radiative nucleon captures for stellar nucleosynthesis. Phys. Rev. C **91**, 044318 (2015). https://doi.org/10.1103/PhysRevC.91.044318
37. A. Tonchev, N. Tsoneva, C. Bhatia et al., Pygmy and core polarization dipole modes in ^{206}Pb: connecting nuclear structure to stellar nucleosynthesis. Phys. Lett. B **773**, 20–25 (2017). https://doi.org/10.1016/j.physletb.2017.07.062
38. S.F. Semenko, Sov. J. Nucl. Phys. **34**, 356 (1981)
39. A. Repko, V.O. Nesterenko, J. Kvasil, P.G. Reinhard, Systematics of toroidal dipole modes in Ca, Ni, Zr, and Sn isotopes. Eur. Phys. J. A **55**, 242 (2019). https://doi.org/10.1140/epja/i2019-12770-x
40. M. Spieker et al., Accessing the single-particle structure of the Pygmy Dipole Resonance in ^{208}Pb. Phys. Rev. Lett. **125**, 102593 (2020). https://doi.org/10.1103/PhysRevLett.125.102503
41. M. Weinert et al., Microscopic structure of the low-energy electric dipole response of ^{120}Sn. Phys. Rev. Lett. **127**, 242501 (2021). https://doi.org/10.1103/PhysRevLett.127.242501
42. A. Zilges, D.L. Balabanski, J. Isaak, N. Pietralla, Photonuclear reactions-from basic research to applications. Prog. Part. Nucl. Phys. **122**, 103903 (2022). https://doi.org/10.1016/j.ppnp.2021.103903
43. P. von Neumann-Cosel, A. Tamii, Electric and magnetic dipole modes in high-resolution inelastic proton scattering at 0°. Eur. Phys. J. A **55**, 110 (2019). https://doi.org/10.1140/epja/i2019-12781-7
44. D. Savran et al., Multi-messenger investigation of the Pygmy Dipole Resonance in ^{140}Ce. Phys. Lett. B **786**, 16 (2018). https://doi.org/10.1016/j.physletb.2018.09.025
45. J. Enders et al., Isospin character of the Pygmy Dipole Resonance in ^{124}Sn. Phys. Rev. Lett. **105**, 212503 (2010). https://doi.org/10.1103/PhysRevLett.105.212503
46. D. Savran et al., Nature of the Pygmy Dipole Resonance in ^{140}Ce studied in $(\alpha,\alpha\,'\,\gamma)$ experiments. Phys. Rev. Lett. **97**, 172502 (2006). https://doi.org/10.1103/PhysRevLett.97.172502
47. V. Derya et al., Isospin properties of electric dipole excitations in ^{48}Ca. Phys. Lett. B **730**, 288 (2014). https://doi.org/10.1016/j.physletb.2014.01.050
48. L. Pellegri et al., Pygmy dipole resonance in ^{124}Sn populated by inelastic scattering of ^{17}O. Phys. Lett. B **738**, 519 (2014). https://doi.org/10.1016/j.physletb.2014.08.029
49. F.C.L. Crespi et al., Isospin character of low-lying Pygmy Dipole states in ^{208}Pb via inelastic scattering of ^{17}O ions. Phys. Rev. Lett. **113**, 012501 (2014). https://doi.org/10.1103/PhysRevLett.113.012501
50. M. Scheck et al., Investigating the Pygmy Dipole Resonance Using β Decay. Phys. Rev. Lett. **116**, 132501 (2016). https://doi.org/10.1103/PhysRevLett.116.132501
51. B. Löher et al., The decay pattern of the Pygmy Dipole Resonance of ^{140}Ce. Phys. Lett. B **756**, 72 (2016). https://doi.org/10.1016/j.physletb.2016.02.042
52. A.M. Lane, Partial width correlations and common doorway states. Ann. Phys. (N.Y.) **63**, 171 (1971). https://doi.org/10.1016/0003-4916(71)90300-9
53. C. Robin, E. Litvinova, AIP Conf. Proc. **1912**, 020014 (2017). https://doi.org/10.1063/1.5016139
54. O. Wieland et al., Search for the Pygmy Dipole Resonance in ^{68}Ni at 600 MeV per nucleon. Phys. Rev. Lett. **102**, 092502 (2009). https://doi.org/10.1103/PhysRevLett.102.092502
55. M. Assie et al., The MUGAST-AGATA-VAMOS campaign: set-up and performances. Nucl. Instr. Methods Phys. Res. **A1014**, 165743 (2021). https://doi.org/10.1016/j.nima.2021.165743
56. GRIT web page. http://grit.in2p3.fr
57. J.-J. Dormard et al., Pulse shape discrimination for GRIT: beam test of a new integrated charge and current preamplifier coupled with high granularity Silicon detectors. Nucl. Instr. Methods Phys. Res. **A1013**, 165641 (2021). https://doi.org/10.1016/j.nima.2021.165641
58. A. Andrigetto et al., Production of high-intensity RIB at SPES. Nucl. Phys. A **834**, 754 (2010). https://doi.org/10.1016/j.nuclphysa.2010.01.137
59. F. Naqvia et al., Developement of slowed down beams at the fragment separator for FAIR. Act. Phys. Pol. B **42**, 725 (2011). https://doi.org/10.5506/APhysPolB.42.725
60. A. Schiller et al., Extraction of level density and gamma strength function from primary gamma spectra. Nucl. Instr. Methods Phys. Res. **A447**, 498 (2000). https://doi.org/10.1016/S0168-9002(99)01187-0
61. A.-C. Larsen et al., Analysis of possible systematic errors in the Oslo method. Phys. Rev. C **83**, 034315 (2011). https://doi.org/10.1103/PhysRevC.83.034315
62. M. Guttormsen et al., The unfolding of continuum gamma-ray spectra. Nucl. Instrum. Methods Phys. Res. Sect. A. **374**, 371 (1996). https://doi.org/10.1016/0168-9002(96)00197-0

63. V. W. Ingeberg et al. "The Oslo Scintilator Detector Array" in preparation
64. M. Markova et al., Nuclear level densities and γ-ray strength functions in 120,124Sn isotopes: impact of porter-Thomas fluctuations. Phys. Rev. C **106**, 034322 (2022). https://doi.org/10.1103/PhysRevC.106.034322
65. M. Markova et al., Comprehensive test of the Brink-Axel Hypothesis in the energy region of the Pygmy Dipole Resonance. Phys. Rev. Lett. **127**, 182501 (2021). https://doi.org/10.1103/PhysRevLett.127.182501
66. L. Wolfenstein, Conservation of angular momentum in the statistical theory of nuclear reactions. Phys. Rev. **82**, 690–696 (1951). https://doi.org/10.1103/PhysRev.82.690
67. W. Hauser, H. Feshbach, The inelastic scattering of neutrons. Phys. Rev. **87**, 366–373 (1952). https://doi.org/10.1103/PhysRev.87.366
68. A. J. Koning, S. Hilaire, and M. C. Duijvestijn, TALYS- 1.0, in ND2007 (EDP Sciences, Les Ulis, France, 2007) pp. 211–214
69. I.K.B. Kullmann et al., First experimental constraint on the Os-191(n, gamma) reaction rate relevant to s-process nucleosynthesis. Phys. Rev. C **99**, 065806 (2019). https://doi.org/10.1103/PhysRevC.99.065806
70. F. Pogliano et al., Indirect measurement of the (n, gamma) Sb-127 cross section. Phys. Rev. C **106**, 015804 (2022). https://doi.org/10.1103/PhysRevC.106.015804
71. H.T. Nyhus et al., Radiative strength functions in Dy-163, Dy-164. Phys. Rev. C **81**, 024325 (2010). https://doi.org/10.1103/PhysRevC.81.024325
72. K.L. Malatji et al., Statistical properties of the well deformed Sm-153, Sm-155 nuclei and the scissors resonance. Phys. Rev. C **103**, 014309 (2021). https://doi.org/10.1103/PhysRevC.103.014309
73. M. Guttormsen et al., Evolution of the γ-ray strength function in neodymium isotopes. Phys. Rev. C **106**, 034314 (2022). https://doi.org/10.1103/PhysRevC.106.034314
74. M. Guttormsen et al., Constant-temperature level densities in the quasicontinuum of Th and U isotopes. Phys. Rev. C **88**, 024307 (2013). https://doi.org/10.1103/PhysRevC.88.024307
75. M. Guttormsen et al., Experimental level densities of atomic nuclei. Eur. Phys. J. A **51**, 170 (2015). https://doi.org/10.1140/epja/i2015-15170-4
76. M. Guttormsen et al., Observation of large scissors resonance strength in actinides. Phys. Rev. Lett. **109**, 162503 (2012). https://doi.org/10.1103/PhysRevLett.109.162503
77. M. Guttormsen et al., Scissors resonance in the quasicontinuum of Th, Pa, and U isotopes. Phys. Rev. C **89**, 014302 (2014). https://doi.org/10.1103/PhysRevC.89.014302
78. T.G. Tornyi et al., Level density and gamma-ray strength function in the odd-odd Np-238 nucleus. Phys. Rev. C **89**, 044323 (2014). https://doi.org/10.1103/PhysRevC.89.044323
79. T.A. Laplace et al., Statistical properties of Pu-243, and Pu-242(n, gamma) cross section calculation. Phys. Rev. C **93**, 014323 (2016). https://doi.org/10.1103/PhysRevC.93.014323
80. M. Guttormsen et al., Validity of the Generalized Brink-Axel Hypothesis in Np-238. Phys. Rev. Lett. **116**, 012502 (2016). https://doi.org/10.1103/PhysRevLett.116.012502
81. A.J. Koning et al., TENDL: Complete Nuclear Data Library for Innovative Nuclear Science and Technology, Nuclear Data Sheets 155 (2019) https://doi.org/10.1016/j.nds.2019.01.002
82. O. Iwamoto et al., Status of JENDL, EPJ Web of Conferences vol. **239**, (2020) https://doi.org/10.1051/epjconf/202023909002
83. A.J.M. Plompen et al., The joint evaluated fission and fusion nuclear data library, JEFF-3.3. Eur. Phys. J. A (2020). https://doi.org/10.1140/epja/s10050-020-00141-9
84. A. Voinov et al., Large enhancement of radiative strength for soft transitions in the quasicontinuum. Phys. Rev. Lett. **93**, 142504 (2004). https://doi.org/10.1103/PhysRevLett.93.142504
85. A.-C. Larsen et al., Evidence for the dipole nature of the low-energy gamma enhancement in Fe-56. Phys. Rev. Lett. **111**, 242504 (2013). https://doi.org/10.1103/PhysRevLett.111.242504
86. A.-C. Larsen et al., Enhanced low-energy gamma-decay strength of Ni-70 and its robustness within the shell model. Phys. Rev. C **97**, 054329 (2018). https://doi.org/10.1103/PhysRevC.97.054329
87. M. Guttormsen et al., Radiative strength functions in Mo93-98. Phys. Rev. C **71**, 044307 (2005). https://doi.org/10.1103/PhysRevC.71.044307
88. A.C. Larsen, S. Goriely, Impact of a low-energy enhancement in the gamma-ray strength function on the neutron-capture cross section. Phys. Rev. C **82**, 014318 (2010). https://doi.org/10.1103/PhysRevC.82.014318
89. V.W. Ingeberg et al., First application of the Oslo method in inverse kinematics. Eur. Phys. J. A **56**, 68 (2020). https://doi.org/10.1140/epja/s10050-020-00070-7
90. A. Spyrou et al., Novel technique for constraining r-process (n, gamma) reaction rates. Phys. Rev. Lett. **113**, 232502 (2014). https://doi.org/10.1103/PhysRevLett.113.232502
91. F.B. Zeiser et al., Restricted spin-range correction in the Oslo method: the example of nuclear level density and gamma-ray strength function from Pu-239(d, p gamma)Pu-240. Phys. Rev. C **100**, 024305 (2019). https://doi.org/10.1103/PhysRevC.100.024305
92. J. Piekarewicz, Unmasking the nuclear matter equation of state. Phys. Rev. C **69**, 041301(R) (2004). https://doi.org/10.1103/PhysRevC.69.041301
93. P.F. Bortignon, A. Bracco, R.A. Broglia, Giant Resonances. Nuclear structure at finite temperature, contemporary concepts in physics, vol. **10**, Harwood Academic Publisher, ISBN 90-5702-570-1
94. W.L. Lv, Y.F. niu, G. Colo, Learning about the structure of giant resonances from their γ decay. Phys. Rev. C **103**, 064321 (2021). https://doi.org/10.1103/PhysRevC.103.064321
95. Y.K. Gupta et al., Deformation effects on isoscalar giant resonances in 24Mg. Phys. Rev. C **93**, 044324 (2016). https://doi.org/10.1103/PhysRevC.93.044324
96. J. Beene et al., Heavy-ion excitation and photon decay of giant resonances in ^{208}Pb. Phys. Rev. C **39**, 1307 (1989). https://doi.org/10.1103/PhysRevC.39.1307
97. B. Wasilewska et al., γ decay to the ground state from the excitations above the neutron threshold in the ^{208}Pb(p, p'γ) reaction at 85 MeV. Phys. Rev. C **105**, 014310 (2022). https://doi.org/10.1103/PhysRevC.105.014310
98. A. Tamii et al., Complete electric dipole response and the neutron skin in ^{208}Pb. Phys. Rev. Lett. **107**, 062502 (2011). https://doi.org/10.1103/PhysRevLett.107.062502
99. M. Ciemala et al., Acta Phys. Pol. B Proc. Suppl. **16**, 4–A3 (2023)
100. S. Mukhopadhyay et al., Coexisting shape- and high-K isomers in the shape transitional nucleus ^{188}Pt. Phys. Lett. B **739**, 462 (2014). https://doi.org/10.1016/j.physletb.2014.10.069
101. M. Kmiecik et al., Probing nuclear shapes close to the fission limit with the giant dipole resonance in ^{216}Rn. Phys. Rev. C **70**, 064317 (2004). https://doi.org/10.1103/PhysRevC.70.064317
102. F. Camera et al., The γ-decay of the GDR built on superdeformed states in ^{143}Eu. EPJ **A2**, 1 (1998)
103. F. Camera, Gamma decay of the giant dipole resonance and feeding of superdeformed states in Eu-143. Phys. At. Nucl. **64**, 1039 (2001). https://doi.org/10.1134/1.1383613
104. G. Benzoni et al., Effect of E1 decay in the population of superdeformed structures. Phys. Lett. B **540**, 199 (2002). https://doi.org/10.1016/S0370-2693(02)02175-5
105. B. Herskind, Nucl. Phys. **447**, 395 (1986). (**and references therein**)

106. A. Maj et al., Angular distribution of photons from the delay of the GDR in hot and rotating light Yb nuclei from exclusive experiments. Nucl. Phys. A **571**, 185 (1994). https://doi.org/10.1016/0375-9474(94)90347-6
107. G. de Angelis, A. Bracco, D. Curien, The EUROBALL gamma ray detector array. Europhys. News (2003). https://doi.org/10.1051/epn:2003503. (**and references therein**)
108. A. Bracco, F. Camera, S. Leoni, Gamma decay of the GDR on superdeformed configurations of ^{143}Eu. Nucl. Phys. A **682**, 449c (2001). https://doi.org/10.1016/S0375-9474(00)00672-2
109. B. Herskind et al., Population and Decay of the superdeformed rotational band of ^{152}Dy. Phys. Rev. Lett. **59**, 2416 (1987). https://doi.org/10.1103/PhysRevLett.59.2416
110. E. Gamba private communications
111. S. Cohen, F. Plasil, W.J. Świątecki, Equilibrium configurations of rotating charged or gravitating liquid masses with surface tension. II. Ann. Phys. (NY) **82**, 557 (1974). https://doi.org/10.1016/0003-4916(74)90126-2
112. K. Pomorski, J. Dudek, Nuclear liquid-drop model and surface-curvature effects. Phys. Rev. C **67**, 044316 (2003). https://doi.org/10.1103/PhysRevC.67.044316
113. M. Kicinska-Habior et al., Search for a phase transition in the nuclear shape at finite temperature and rapid rotation. Phys. Lett. B **308**, 225 (1993). https://doi.org/10.1016/0370-2693(93)91276-S
114. A. Maj et al., Evidence for the Jacobi shape transition in hot ^{46}Ti. Nucl. Phys. A **731**, 319 (2004). https://doi.org/10.1016/j.nuclphysa.2003.11.043
115. D. Pandit et al., Extreme nuclear shapes examined via giant dipole resonance lineshapes in hot light-mass systems. Phys. Rev. C **81**, 061302(R) (2010). https://doi.org/10.1103/PhysRevC.81.061302
116. B. Dey et al., Study of the Jacobi shape transition in A≈30 nuclei. Phys. Rev. C **97**, 014317 (2018). https://doi.org/10.1103/PhysRevC.97.014317
117. M. Kmiecik et al., Acta Phys. Pol. B **36**, 1159 (2005)
118. B. Herskind et al., Acta Phys. Pol. B **38**, 1421 (2007)
119. A. Maj, S. Leoni, Letter of Intent "Study of collective modes of excitations in the neutron rich Ba region via fusion-evaporation reactions", Day 1 SPIRAL2 Phase 2
120. A. Maj, K. Mazurek, J. Dudek, M. Kmiecik, D. Rouvel, Shape evolution at high spins and temperatures: nuclear Jacobi and Poincare transitions. Int. J. Mod. Phys. E **19**, 532 (2010). https://doi.org/10.1142/S0218301310014947
121. V.G. Soloviev, *Theory of Atomic Nuclei: Quasiparticles and Phonons* (Institute of Physics, Bristol, 1992)